Soft Matter

ROYAL SOCIETY OF CHEMISTRY

PAPER

View Article Online
View Journal | View Issue

Cite this: *Soft Matter*, 2022, **18**, 3218

Mechanochromic elastomers with different thermo- and mechano-responsive radical-type mechanophores†

Kosaku Yanada, Daisuke Aoki and Hideyuki Otsuka *

To design tough soft materials, the introduction of sacrificial bonds into their skeleton is a useful method. The introduction of radical-type mechanophores (RMs), which generate coloured radicals in response to mechanical stimuli, as sacrificial bonds into the cross-linking points of elastomers is expected to be a powerful tool to elucidate the fracture mechanisms as well as the toughening of materials, given that the radicals generated from the RMs are coloured and can be quantitatively evaluated using electron paramagnetic resonance (EPR) measurements. In this study, to investigate the effect of the dynamic nature, *i.e.*, the reactivity, of RMs introduced at the cross-linking points of polymer networks on their macroscopic mechanical properties, polymer networks cross-linked by two different RMs, a symmetric radical-type mechanophore (DFSN) and a non-symmetric radical-type mechanophore (CF/ABF), were synthesized and characterized. Compared to the polymer network cross-linked by DFSN, the network with CF/ABF exhibited higher thermal and mechanical responses, in other words much more sensitive to heat and mechanical force, resulting in better stress relaxation and energy-dissipation properties. These results demonstrate that the reactivity of the radical mechanophore at the cross-linking point is an important factor for designing polymer networks.

Received 20th December 2021,
Accepted 17th March 2022

DOI: 10.1039/d1sm01786a

rsc.li/soft-matter-journal

Introduction

Biological materials, such as nacre, bones in mammals and spider silk, are known for their extraordinary stiffness, strength, and toughness, as well as their self-healing ability.[1–3] These properties are attributed to sacrificial bonds and hidden length, which break and dissipate energy prior to the fracture of the main chain under stress. Inspired by this concept, several materials with significant improvements in stiffness, strength, toughness, fatigue resistance and self-healing properties have been reported.[4–7] Hydrogen bonds,[8] metal–ligand coordination bonds[9] and ionic bonds[10] are commonly used as sacrificial bonds. In pioneering work on the use of covalent bonds as sacrificial bonds, Gong *et al.* developed a high-strength and high-toughness double-network gel consisting of a hard and brittle primary network and a soft and flexible secondary network.[11–13] The fracture of the primary network dissipates the energy applied to the material, while the elasticity of the secondary network maintains the original shape. Creton *et al.* developed double- and triple-network elastomers with a chemiluminescent dioxetane cross-linker, which allowed mapping of when and where the bonds break before crack propagation in real time.[14] The chemiluminescent cross-linker, which acts as a mechanophore in their research, serves multiple purposes, such as sacrificial bonding and luminescence probe behaviour, leading to the elucidation of the fracture mechanism as well as the toughening of the materials. However, since these irreversible covalent sacrificial bonds are quickly deactivated upon cleavage, it is difficult to evaluate their effect on the macroscopic properties in soft materials, especially in elastomers. Weng *et al.* achieved mechanochromic and energy dissipation properties in elastomers by introducing anthracene dimers at the cross-linking points and also achieved repeatability *via* the reformation of the dimers upon UV irradiation.[15]

Our group has reported various types of elastomers with the radical-type mechanophore (RM)[16–19] difluorenylsuccinonitrile (DFSN), which generates relatively stable radicals in response to mechanical stimuli as a sacrificial cross-linker (Fig. 1a). Since the radicals generated from DFSN are pink and relatively stable in a network structure, they have been used to evaluate energy dissipation properties under stress *via* not only the change in coloration, but also the quantitative evaluation of the radicals using electron paramagnetic resonance (EPR) measurements.[20–24]

Department of Chemical Science and Engineering, Tokyo Institute of Technology, 2-12-1 Ookayama, Meguro-ku, Tokyo 152-8550, Japan

† Electronic supplementary information (ESI) available: Details of ^{1}H and ^{13}C NMR spectra, GPC profiles, DSC profiles, solid-state UV-vis spectra, EPR spectra and photographs of the synthesized compounds and polymers. See DOI: 10.1039/d1sm01786a

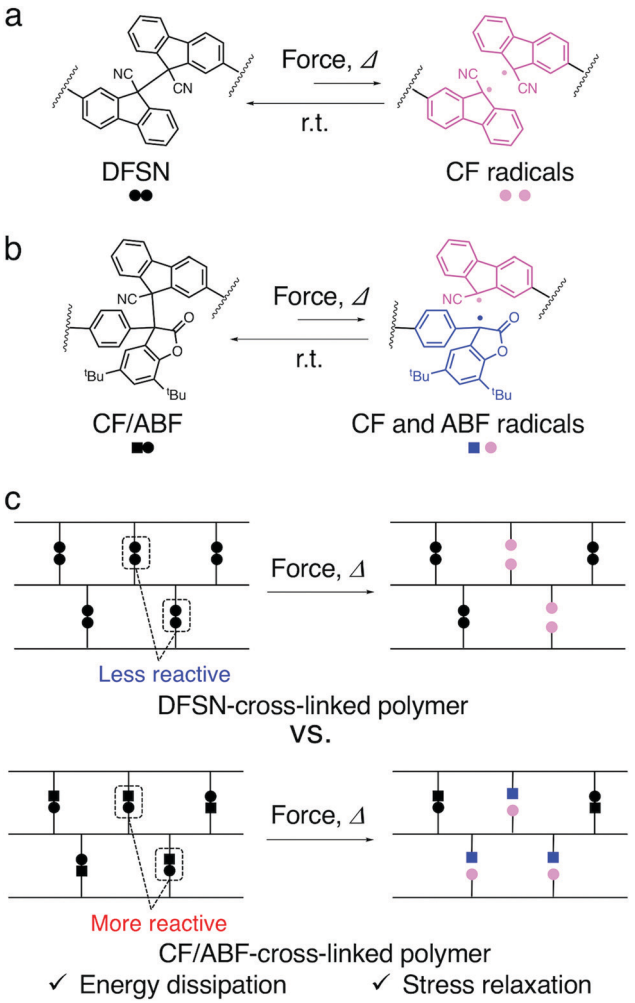

Fig. 1 (a) Equilibrium between DFSN and its radical species. (b) Equilibrium between CF/ABF and its radical species. Illustration of (c) a DFSN-cross-linked polymer and a CF/ABF-cross-linked polymer, as well as the mechanism of energy dissipation and stress relaxation.

Moreover, it can be expected that the generated radicals are able to spontaneously recombine under an ambient atmosphere and reform the original dimer in an appropriate matrix with high mobility, thus leading to the ability to repeatedly dissipate stress.[25–28]

Although there are several examples of cross-linked polymers with dynamic covalent bonds (DCBs) at the cross-linking points, attention has hitherto been focused on their self-healing and reprocessing properties, and there are only a few examples in which their sacrificial bonding properties have been evaluated. In particular, the effect of the dynamic nature, *i.e.*, the reactivity, of DCBs introduced at the cross-linking points on the macroscopic mechanical properties of the polymer due to energy dissipation has not been investigated in detail.

We have recently reported the synthesis of the non-symmetric mechanophore cyanofluorenyl/arylbenzofuranone (CF/ABF; Fig. 1b) *via* a coupling reaction between the cyanofluorene (CF) radical generated from DFSN and the arylbenzofuranone (ABF) radical from another RM, diarylbenzofuranone (DABBF).[16,29] The non-symmetric mechanophore CF/ABF produces two different radical species (CF and ABF radicals), which are pink and blue, respectively, in response to mechanical stimuli to show mixed mechanochromism, *i.e.*, a purple coloration that is a mixture of pink and blue. Furthermore, the thermal and mechanical responsiveness of CF/ABF is higher than that of DFSN.[29] In this paper, we report the synthesis of cross-linked polymers with two types of RMs at the cross-linking points that show different mechano- and thermo-reactivity, *i.e.*, polymers with DFSN and CF/ABF as the cross-linkers, and investigate the effects of these RMs on the mechanical properties of the polymers (Fig. 1c). Namely, a series of poly(*n*-hexyl methacrylate) (PHMA) networks with 1 mol% DFSN or CF/ABF at the cross-linking points were synthesized *via* radical polymerization. As a control sample, PHMA cross-linked using the same concentration of the conventional cross-linker dimethacrylate was also prepared. The structural formula of the cross-linkers and the synthetic route are shown in Fig. 2. The energy dissipation properties were evaluated using tensile testing, *in situ* EPR measurements, and stress-relaxation measurements.

Experimental

Materials

All reagents and solvents were purchased from Sigma-Aldrich, FUJIFILM Wako Pure Chemical Corporation, Tokyo Chemical Industry and Kanto Chemical, and used as received unless otherwise noted. Hexyl methacrylate (HMA) was purified using a basic alumina column (Merck KGaA) to remove the stabilizer prior to use. **DFSN-dimethacrylate** was synthesized according to previously published methods.[21]

Measurements

^{1}H NMR spectroscopy measurements were carried out using a 500 MHz Bruker spectrometer with tetramethylsilane (TMS) as the internal standard in chloroform-*d* ($CDCl_3$). Electrospray ionization mass spectrometry (ESI-TOF-MS) measurements were carried out using a Bruker micrOTOF II. IR spectra were recorded on a JASCO FT/IR-4100 Fourier transform infrared spectrometer using thin films with KBr. Size exclusion chromatography (SEC) measurements were carried out at 40 °C on a TOSOH HLC-8320 SEC system equipped with a guard column (TOSOH TSK guard column Super H-L), three columns (TOSOH TSK gel SuperH 6000, 4000 and 2500), and a differential refractive index detector. Tetrahydrofuran (THF) was used as the eluent at a flow rate of 0.6 mL min^{-1}. Polystyrene (PS) standards (M_n = 4430–32 42 000; M_w/M_n = 1.03–1.08) were used to calibrate the SEC system. Differential scanning calorimetry (DSC) measurements were carried out using a SHIMADZU DSC-60A Plus with a heating rate of 10 °C min^{-1}. Uniaxial tensile tests were performed using a SHIMADZU AUTOGRAPH AGS-X with a constant-temperature bath TCE-N300. Stress relaxation

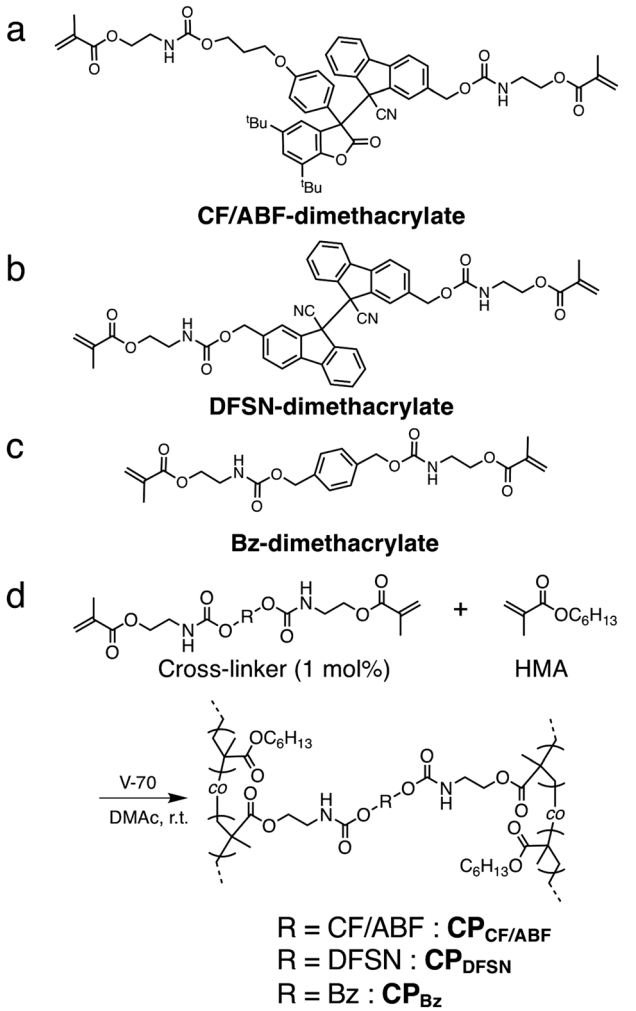

Fig. 2 Chemical structures of (a) CF/ABF-dimethacrylate, (b) DFSN-dimethacrylate and (c) Bz-dimethacrylate. (d) Synthetic route to $\mathbf{CP_{CF/ABF}}$, $\mathbf{CP_{DFSN}}$ and $\mathbf{CP_{Bz}}$.

measurements were carried out using a Hitachi High-Tech Science TMA7100 under a N_2 flow.

Stress-relaxation measurements

The sample films (10 mm × 3 mm × 0.7–0.8 mm) were equilibrated at a set temperature for 10 min and then held at 3% strain with an initial elongation speed of 3% s^{-1}, after which the decay of stress over time was monitored.

Uniaxial tensile tests

The tests were performed with ISO 37-4 specimens (12 mm × 2 mm × 0.7–0.8 mm) punched out from films of $\mathbf{CP_{CF/ABF}}$, $\mathbf{CP_{DFSN}}$ and $\mathbf{CP_{Bz}}$, which were stretched at a strain rate of 100 mm min^{-1}. The measurements were performed three times for each test, based on which the average values with standard error were calculated.

EPR spectroscopy during uniaxial tensile deformation

Electron paramagnetic resonance (EPR) measurements of **CPCF/ABF** and **CPDFSN** during uniaxial tensile deformation were carried out using a JEOL JES-F A200 EPR X-band spectrometer equipped with a Baldwin tensile tester using strip specimens (100 mm × 3–4 mm × 0.7–0.8 mm). The effective measuring range was 43.5 mm in height. The specimens were stretched to 25, 50, 75, 100, 125, 150, 175, 200, 225, 250, 275, 300, 325, 350, 375 and 400% strain sequentially at a strain rate of 100 mm min^{-1}. The EPR spectra were measured at each strain at r.t. using a microwave power of 0.998 mW, a field modulation of 0.1 mT with a time constant of 0.03 s and a sweep rate of 0.75 mT s^{-1}. The concentrations of radicals formed from the cleavage of DABBF, DFSN and CF/ABF were determined by comparing the area of the integral of the spectrum with a 0.05 mM solution of 4-hydroxy-2,2,6,6-tetramethylpiperidin-1-oxyl (TEMPOL) in benzene under the same experimental conditions. The Mn^{2+} signal was used as an auxiliary standard. The g value was calculated according to the equation $g = h\nu/\beta H$, where h is the Planck constant, ν is the microwave frequency, β is the Bohr magneton and H is the magnetic field.

VT-EPR spectroscopy of CP_x

Variable-temperature EPR measurements of $\mathbf{CP_x}$ were carried out using a JEOL JES-X320 X-band EPR spectrometer equipped with a JEOL DVT temperature controller. The samples (3 mm × 3 mm × 0.7–0.8 mm) were taken in 5 mm glass capillaries, which were sealed after being degassed. The spectra were measured using a microwave power of 1.0 mW, a field modulation of 0.1 mT with a time constant of 0.03 s and a sweep rate of 0.25 mT s^{-1} during the heating process from 120 to 160 °C. The concentrations of the radicals formed from the cleavage of DFSN and CF/ABF were determined by comparing the area of the integral of the spectrum with a 0.05 mM solution of TEMPOL in benzene under the same experimental conditions. The Mn^{2+} signal was used as an auxiliary standard. The g value was calculated according to the equation $g = h\nu/\beta H$, where h is the Planck constant, ν is the microwave frequency, β is the Bohr magneton and H is the magnetic field.

Synthesis of DABBF-diOTBS

In a round-bottomed flask, a solution of DABBF-diol (2.00 g, 2.53 mmol), imidazole (0.52 g, 7.58 mmol) and *N*,*N*-dimethylformamide (DMF, 70 mL) was prepared under a N_2 atmosphere. A solution of *tert*-butyldimethylsilyl chloride (TBSCl, 1.15 g, 7.58 mmol) and dichloromethane (20 mL) was added dropwise to this mixture at 0 °C. The reaction mixture was stirred at room temperature for 2 h and then poured into water. The reaction mixture was extracted with ethyl acetate, the organic layer was washed with brine and dried over anhydrous $MgSO_4$, and the solvent was removed. The crude product was purified by column chromatography on silica gel (eluent: ethyl acetate/*n*-hexane = 1/9, v/v). The solvent was removed

under reduced pressure and the residue was dried under vacuum to give **DABBF-diOTBS** as a white solid (2.12 g, 83%).

Synthesis of HO-CF/ABF-OTBS

In a round-bottomed flask, a solution of **DFSN-diol** (0.90 g, 2.04 mmol), **DABBF-diOTBS** (2.08 g, 2.04 mmol) and 1,4-dioxane (300 mL) was prepared. The mixture was sparged with nitrogen for 1 h. The reaction mixture was stirred at 90 °C for 3 h. The crude product was purified *via* column chromatography on silica gel (eluent: ethyl acetate/*n*-hexane = 1/4, v/v). The solvent was removed under reduced pressure and the residue was dried *in vacuo* to give **HO-CF/ABF-OTBS** as a white solid (1.76 g, 59%).

Synthesis of CF/ABF-diol

A round-bottomed flask was charged with a solution of **HO-CF/ABF-OTBS** (0.70 g, 0.96 mmol), 1N HCl (2.9 mL) and tetrahydrofuran (70 mL). The reaction mixture was stirred at r.t. for 1 h. Then, the reaction mixture was quenched with water and extracted with ethyl acetate; the organic layer was washed with brine, dried over anhydrous $MgSO_4$, and filtered, and the solvent was removed under reduced pressure. The crude product was purified by column chromatography on silica gel (eluent: ethyl acetate/*n*-hexane = 1/4, v/v). The solvent was removed under reduced pressure and the residue was dried *in vacuo* to give **CF/ABF-diol** as a white solid (0.51 g, 87%).

Synthesis of CF/ABF-dimethacrylate

CF/ABF-diol (1.06 g, 1.72 mmol) was added to a sample tube. After a N_2 purge, tetrahydrofuran (THF) (10 mL), 2-isocyanatoethyl methacrylate (0.82 mL, 6.02 mmol) and di-*n*-butyltin dilaurate (DBTDL; 1 drop) were added to the mixture, which was then stirred for 3 h at room temperature. The crude product was quenched with water and extracted with ethyl acetate; the organic layer was washed with brine, dried over anhydrous $MgSO_4$, and filtered, and the solvent was removed under reduced pressure. The crude product was purified by column chromatography on silica gel (eluent: ethyl acetate/*n*-hexane = 1/1, v/v). The solvent was removed under reduced pressure and the residue was dried *in vacuo* to give **CF/ABF-dimethacrylate** as a white solid (1.33 g, 85%).

Preparation of the PHMA films *via* free radical polymerization

Typical method: A solution of HMA (2.21 g, 13.0 mmol), **CF/ABF-dimethacrylate** (120 mg, 0.130 mmol), 2,2′-azobis(4-methoxy-2,4-dimethylvaleronitrile) (V-70, 40.0 mg, 0.13 mmol) and dry *N*,*N*-dimethylacetamide (DMAc, 2.33 g, *ca.* 50 wt%) was degassed using three freeze–pump–thaw cycles. After 15 minutes of stirring at 25 °C ± 5 °C, the solution was transferred *via* a syringe into a Petri dish inside a N_2-filled separable flask and left to react for 48 hours. The reaction was quenched by exposure to air, and the obtained polymer film was washed with a mixture of chloroform/methanol (gradient from 1/1 to 1/3) several times. The washed film was dried at room temperature for 12 h and then *in vacuo* at elevated temperatures (gradually increasing from 25 °C to 40 °C) to afford a colourless film of $\mathbf{CP_{CF/ABF}}$ (2.21 g, 92% yield).

Results and discussion

The CF/ABF cross-linker was synthesized by a reaction of a CF/ABF diol derivative (**CF/ABF-diol**) with 2-isocyanatoethyl methacrylate (Scheme 1). **CF/ABF-diol** was prepared by deprotection of **HO-CF/ABF-OTBS**, which was synthesized by a radical exchange reaction between hydroxylated DFSN (**DFSN-diol**) and TBS-protected DABBF (**DABBF-diOTBS**). DABBF was temporarily protected because the resulting non-symmetric RMs cannot be isolated *via* column chromatography unless there is a difference in polarity between the parent molecules. The obtained cross-linker was characterized using ^{1}H NMR, ^{13}C NMR, and FT-IR spectroscopy, as well as ESI-TOF-MS, which supported the successful synthesis of **CF/ABF-dimethacrylate** (Fig. S1–S4, ESI†). A control cross-linker with a benzene

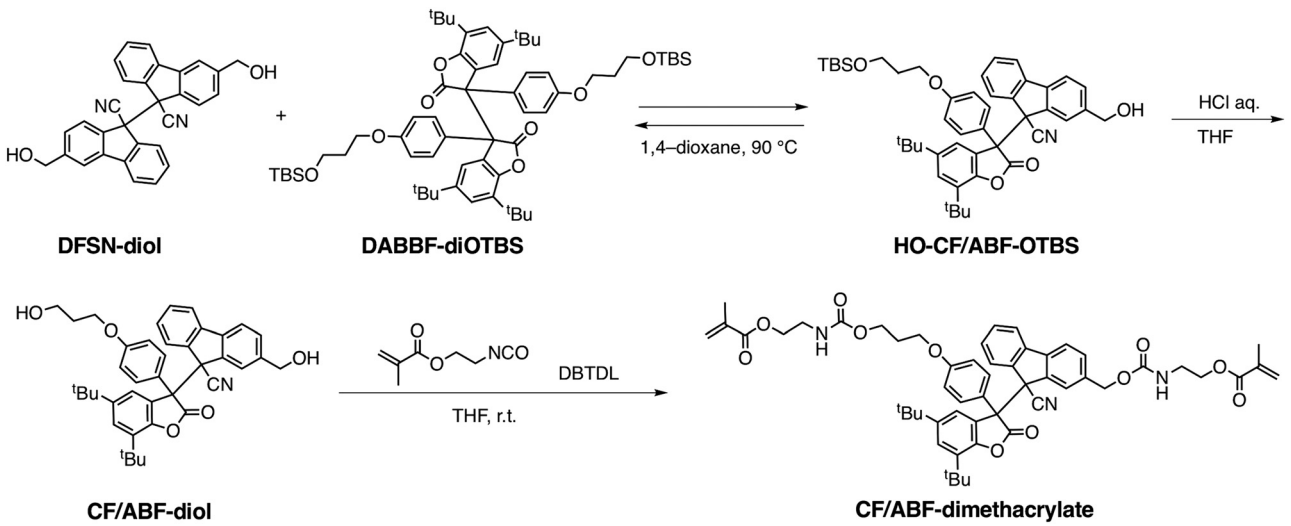

Scheme 1 Synthetic route to the CF/ABF cross-linker (**CF/ABF-dimethacrylate**).

skeleton at the center, **BF-dimethacrylate**, was also synthesized using a similar method (Fig. S5, ESI†), and the DFSN cross-linker, **DFSN-dimethacrylate**, was synthesized as previously reported.[21]

The cross-linked polymer films were prepared *via* the free radical polymerization of *n*-hexyl methacrylate in the presence of the cross-linkers (Fig. 2d). Poly(*n*-hexyl methacrylate) (PHMA) was selected as the matrix polymer because it is elastic at room temperature given that its glass-transition temperature (T_g) is lower than room temperature, and is suitable for tensile testing. It should be noted that the recombination of the generated radicals upon exposure to mechanical stimuli can be sufficiently suppressed by the network structure of PHMA, which is amorphous, but its T_g is relatively close to room temperature, enabling EPR measurements on a time scale of hours. The cross-linker to monomer ratio was set to 1 mol% in all samples. The obtained films were colourless, transparent and insoluble in common organic solvents, indicating cross-linked polymers. All the cross-linked polymers were synthesized in relatively high yields (88–92%; Table S1, ESI†), suggesting that the RM-based cross-linker **CF/ABF-dimethacrylate** did not inhibit the radical polymerization under the applied conditions. It should be noted that DABBF, the parent molecule of CF/ABF, cannot be introduced into the cross-linked polymer *via* free radical polymerization because it acts as a polymerization inhibitor.[30] By improving the thermal stability through molecular cross-linking with DFSN, we succeeded in introducing the source of the DABBF-derived radical (ABF radical) species into the cross-linking point. Hereafter, the cross-linked polymers are referred to as $\mathbf{CP}_x$, where x is the cross-linker. The thermal properties of the synthesized $\mathbf{CP}_x$ were evaluated using DSC measurements, which indicated insignificant differences ($\mathbf{CP}_{\mathbf{CF/ABF}}$: −3.6 °C; $\mathbf{CP}_{\mathbf{DFSN}}$: −3.6 °C; $\mathbf{CP}_{\mathbf{Bz}}$: −3.9 °C) in their T_g values (Fig. S6 and Table S1, ESI†). The cross-linking density of $\mathbf{CP}_x$ was characterized using a swelling test. $\mathbf{CP}_x$ films were immersed in a good solvent (anisole) and allowed to swell sufficiently; the swelling degree was then calculated from the weight ratio before and after swelling. The swelling degrees of all samples were almost identical at room temperature (Table S1, ESI†), indicating similar cross-linking densities for all $\mathbf{CP}_x$ films.

$\mathbf{CP}_{\mathbf{CF/ABF}}$ and $\mathbf{CP}_{\mathbf{DFSN}}$ can be de-cross-linked by adding excess low-molecular-weight DFSN and heating, which facilitates characterization of the obtained network structure. Specifically, the insoluble polymer network films were de-cross-linked and converted to linear polymers by adding **DFSN-diol** (∼30 eq.) and heating them to 100 °C. While $\mathbf{CP}_{\mathbf{DFSN}}$ was de-cross-linked in approximately 24 hours, surprisingly, $\mathbf{CP}_{\mathbf{CF/ABF}}$ underwent rapid de-cross-linking within 1 hour (Fig. S7, ESI†). We attributed the rapid de-cross-linking reaction to the high thermal responsiveness of CF/ABF; it is estimated to be 200 times more responsive than DFSN[29] based on the amounts of radicals detected in EPR measurements at 100 °C. Based on GPC measurements, there is almost no difference between the number-average molecular weight (M_n) values of the obtained de-cross-linked polymers of $\mathbf{CP}_{\mathbf{CF/ABF}}$ and $\mathbf{CP}_{\mathbf{DFSN}}$ (Fig. S8, ESI†), indicating that polymerization proceeded regardless of the type of cross-linker used. Furthermore, the cross-linking densities calculated from the ^{1}H NMR measurements of the obtained de-cross-linked polymers were 0.67 mol% for $\mathbf{CP}_{\mathbf{CF/ABF}}$ and 0.70 mol% for $\mathbf{CP}_{\mathbf{DFSN}}$, indicating that polymer network films with an almost equal cross-linking density were synthesized (Fig. S9 and S10, ESI†).

In order to evaluate the exchange ability of the RMs in the obtained $\mathbf{CP}_x$, stress-relaxation measurements were performed

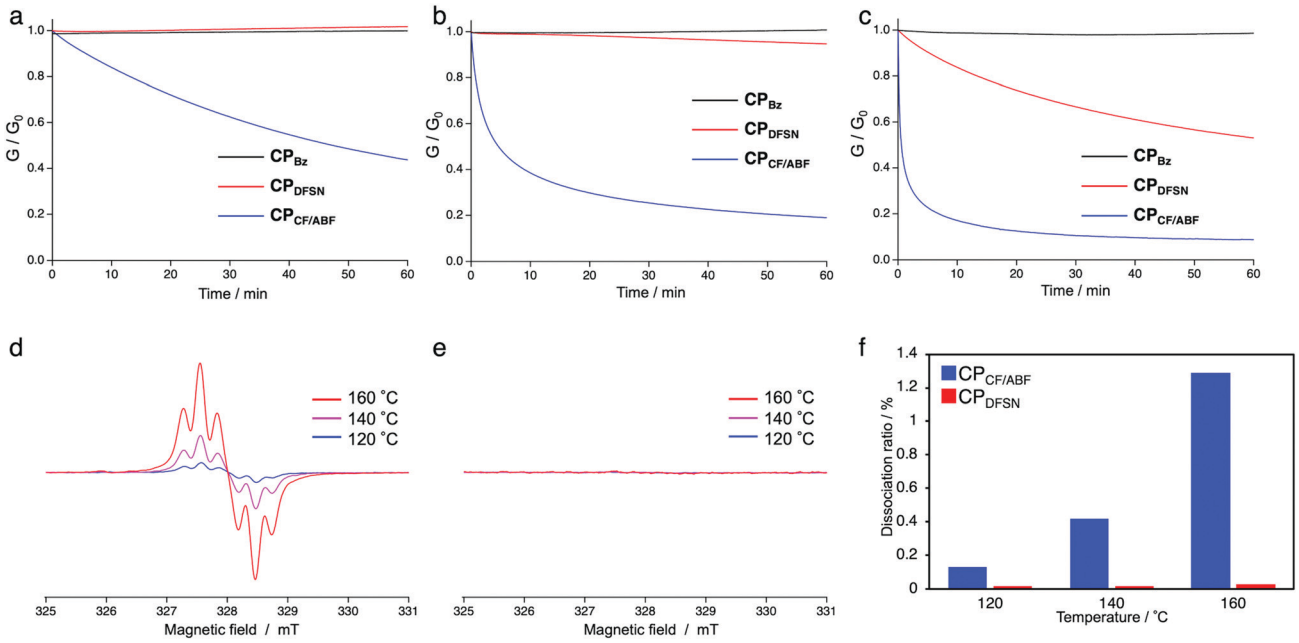

Fig. 3 Stress-relaxation behavior of $\mathbf{CP}_x$ at (a) 120, (b) 140 and (c) 160 °C. EPR spectra of (d) $\mathbf{CP}_{\mathbf{CF/ABF}}$ and (e) $\mathbf{CP}_{\mathbf{DFSN}}$ at 120, 140 and 160 °C. (f) Dissociation ratio of CF/ABF and DFSN in $\mathbf{CP}_{\mathbf{CF/ABF}}$ and $\mathbf{CP}_{\mathbf{DFSN}}$ at 120, 140 and 160 °C.

using thermomechanical analysis (TMA). Rectangular specimens were held at 3% strain at each of the tested temperatures (120, 140 and 160 °C) to dissipate stress (Fig. 3a–c). While **CP_{DFSN}** showed almost no stress relaxation, not even at 140 °C, **$CP_{CF/ABF}$** showed stress relaxation at 120 °C, suggesting that the radical exchange of CF/ABF occurs in a lower temperature range compared to that of DFSN. To confirm that the stress-relaxation behaviour originates from the radical exchange reactions of RMs at the cross-linking points, EPR measurements of the cross-linked films were performed (Fig. 3d–f). The specimens of **CP_{DFSN}** and **$CP_{CF/ABF}$** were placed in sample tubes, and the measurements were performed at 120–160 °C. Carbon-centered radicals were generated in **$CP_{CF/ABF}$** above 120 °C, but not in **CP_{DFSN}**. There is a positive correlation between the amount of radical generation and the degree of stress relaxation, suggesting that the stress relaxation was due to the cleavage of RMs. The better dynamic properties of the cross-linking points under milder conditions, which was attributed to the introduction of the more thermally responsive CF/ABF rather than DFSN, were confirmed in both TMA and EPR measurements.

To confirm the effect of the mechanoresponsiveness of the RMs at the cross-linking points on the macroscopic polymer properties, the mechanical properties of **CP_x** were characterized using uniaxial tensile tests. After fracture in the uniaxial tensile tests, **$CP_{CF/ABF}$** and **CP_{DFSN}** turned purple and pink, respectively, indicating cleavage of the CF/ABF and DFSN at their cross-linking points and the corresponding radical generation (Fig. 4a and b). The degree of visual coloration was higher for **$CP_{CF/ABF}$** than for **CP_{DFSN}**, suggesting that more CF/ABF was cleaved than DFSN, generating a higher concentration of radical species. Furthermore, UV-vis measurements of **$CP_{CF/ABF}$** showed characteristic peaks derived from CF and ABF radicals at 510 nm, 540 nm and 650 nm, confirming the simultaneous generation of different radical species by elongation (Fig. 4d).

In the stress–strain curves, both **$CP_{CF/ABF}$** and **CP_{DFSN}** showed better break elongation, stress and fracture energy than the control sample **CP_{Bz}** with conventional covalent cross-linking points (Fig. 5 and Table 1). However, no significant difference was observed between **$CP_{CF/ABF}$** and **CP_{DFSN}** in uniaxial tensile tests (Fig. S11, ESI†). Therefore, in order to clarify the difference in the mechano-responsivity of **$CP_{CF/ABF}$** and **CP_{DFSN}** in detail, *in situ* EPR measurements of **$CP_{CF/ABF}$** and **CP_{DFSN}** during uniaxial tensile tests were performed. The calculated dissociation ratios of CF/ABF and DFSN in the cross-linked polymers are shown in Fig. 6. Radicals were observed at strains above 300% for **$CP_{CF/ABF}$** and **CP_{DFSN}**, and the concentration of the radicals increased with increasing strain. The concentration of the generated radicals in **$CP_{CF/ABF}$** was 10 times higher than that in **CP_{DFSN}**, which supports the higher mechano-responsivity of CF/ABF and is consistent with the more intense visual coloration. Considering the results of stress–strain curves and the radical generation estimated using EPR for **$CP_{CF/ABF}$** and **CP_{DFSN}**, at strains of up to approximately 300%, the applied stress is mainly dissipated by the entropic elasticity associated with polymer-chain elongation, and the effect of the RMs on the mechanical properties seems to be small. Therefore, the stress–strain curves of both networks are almost identical. On the other hand, in the region

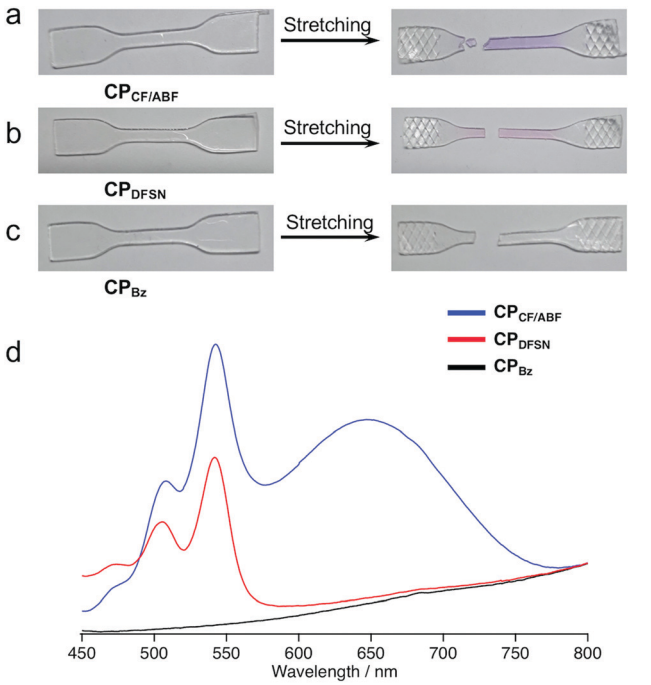

Fig. 4 Photographs of (a) **$CP_{CF/ABF}$**, (b) **CP_{DFSN}** and (c) **CP_{Bz}** films before and after fracture. (d) UV-Vis spectra of **$CP_{CF/ABF}$** (blue), **CP_{DFSN}** (red) and **CP_{Bz}** (black) films after fracture.

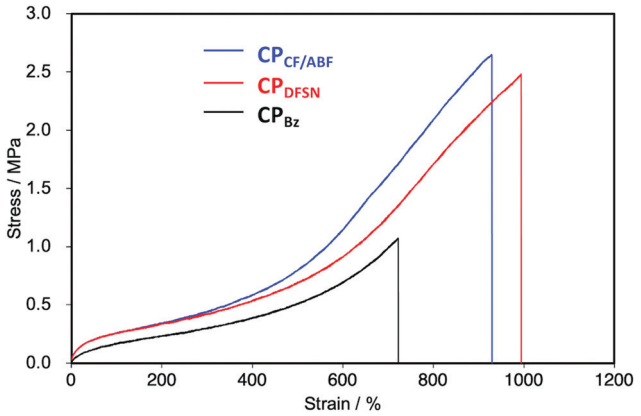

Fig. 5 Stress–strain curves of **$CP_{CF/ABF}$** (blue), **CP_{DFSN}** (red) and **CP_{Bz}** (black) films (100 mm min^{-1}, 30 °C).

Table 1 Results of the tensile tests of **CPCF/ABF**, **CPDFSN** and **CPBz** (100 mm min^{-1}, 30 °C)

Cross-linked polymer	Stress (MPa)	Strain (%)	Fracture energy (MJ m^{-3})
CPCF/ABF	2.50 ± 0.11	915 ± 16	8.74 ± 0.40
CPDFSN	2.45 ± 0.07	958 ± 24	8.97 ± 0.51
CPBz	1.02 ± 0.05	688 ± 28	2.82 ± 0.22

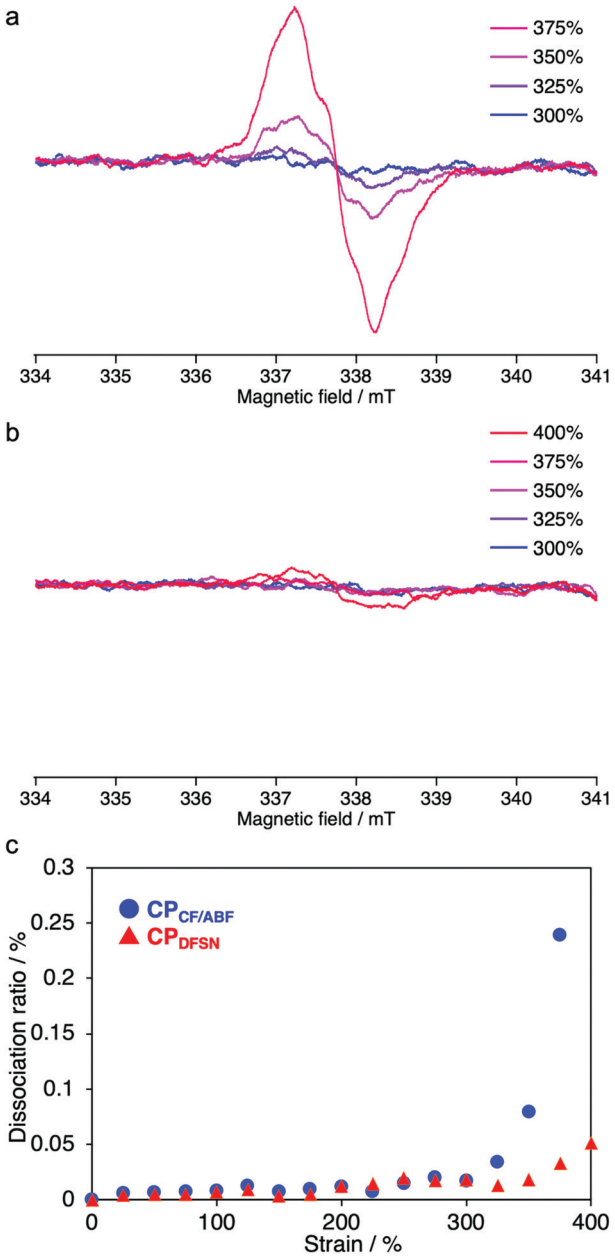

Fig. 6 EPR spectra of (a) $\mathbf{CP_{CF/ABF}}$ and (b) $\mathbf{CP_{DFSN}}$ at each strain (100 mm min^{-1}). Dissociation ratio of the CF/ABF and DFSN moieties of $\mathbf{CP_{CF/ABF}}$ and $\mathbf{CP_{DFSN}}$ at each strain.

above 300%, the number of stretched chains increases, and the stress begins to concentrate at the cross-linking points, causing dissociation of the mechanophores and generation of radical species. Comparison of the amounts of radicals observed in EPR shows a significant difference between $\mathbf{CP_{CF/ABF}}$ (0.03–0.25%) and $\mathbf{CP_{DFSN}}$ (0.01–0.05%), although the significant difference was not observed in the stress–strain curves of $\mathbf{CP_{CF/ABF}}$ and $\mathbf{CP_{DFSN}}$. Further research into the relationship between reactivity and energy-dissipation properties is required to assess sacrificial bonding properties from the viewpoints of material damage.[31]

Conclusions

In this study, to investigate the effect of the reactivity of radical-type mechanophores (RMs) introduced at the cross-linking points on the macroscopic properties of network polymers, we have synthesized and compared polymer network films of poly(*n*-hexyl methacrylate) with the non-symmetric radical-type mechanophore CF/ABF or symmetric radical-type mechanophore DFSN at the cross-linking points. The CF/ABF-cross-linked polymer was much more sensitive to heat and mechanical force than the DFSN-cross-linked polymer, which was attributed to the higher thermal and mechano-responsivity of CF/ABF than that of DFSN. We believe that these results provide a guiding principle for the design of mechanochromic elastomers with various DCBs.

Conflicts of interest

There are no conflicts to declare.

Acknowledgements

This work was supported by KAKENHI grants 17H01205 (H. O.) and 21H04689 (H. O.) from the Japan Society for the Promotion of Science (JSPS), as well as JST CREST grant JPMJCR1991 (H. O.).

Notes and references

1 X. Zhou, B. Guo, L. Zhang and G. H. Hu, *Chem. Soc. Rev.*, 2017, **46**, 6301–6329.
2 J. Sun and B. Bhushan, *RSC Adv.*, 2012, **2**, 7617–7632.
3 M. A. Meyers, J. McKittrick and P.-Y. Chen, *Science*, 2013, **339**, 773–780.
4 B. L. Smith, T. E. Schäffer, M. Vlani, J. B. Thompson, N. A. Frederick, J. Kindt, A. Belcher, G. D. Stucky, D. E. Morse and P. K. Hansma, *Nature*, 1999, **399**, 761–763.
5 Z. Li, J. Wang, X. Li, Y. Wang, L.-J. Fan, S. Yang, M. Guo, X. Li and Y. Tu, *ACS Macro Lett.*, 2020, **9**, 1655–1661.
6 Z. Chen and H. Lu, *J. Mater. Chem.*, 2012, **22**, 12479–12490.
7 H. Chen, F. Yang, Q. Chen and J. Zheng, *Adv. Mater.*, 2017, **29**, 1606900.
8 M. A. Haque, T. Kurokawa and J. P. Gong, *Polymer*, 2012, **53**, 1805–1822.
9 J. A. Neal, D. Mozhdehi and Z. Guan, *J. Am. Chem. Soc.*, 2015, **137**, 4846–4850.
10 Y. Liu, Z. Tang, S. Wu and B. Guo, *ACS Macro Lett.*, 2019, **8**, 193–199.
11 J. P. Gong, Y. Katsuyama, T. Kurokawa and Y. Osada, *Adv. Mater.*, 2003, **15**, 1155–1158.
12 J. P. Gong, *Science*, 2014, **344**, 161–162.
13 T. Matsuda, R. Kawakami, R. Namba, T. Nakajima and J. P. Gong, *Science*, 2019, **363**, 504–508.
14 E. Ducrot, Y. Chen, M. Bulters, R. P. Sijbesma and C. Creton, *Science*, 2014, **344**, 186–189.

15 H. Zhang, D. Zeng, Y. Pan, Y. Chen, Y. Ruan, Y. Xu, R. Boulatov, C. Creton and W. Weng, *Chem. Sci.*, 2019, **10**, 8367–8373.
16 K. Imato, A. Irie, T. Kosuge, T. Ohishi, M. Nishihara, A. Takahara and H. Otsuka, *Angew. Chem., Int. Ed.*, 2015, **54**, 6168–6172.
17 T. Sumi, R. Goseki and H. Otsuka, *Chem. Commun.*, 2017, **53**, 11885–11888.
18 K. Ishizuki, H. Oka, D. Aoki, R. Goseki and H. Otsuka, *Chem. – Eur. J.*, 2018, **24**, 3170–3173.
19 K. Kawasaki, D. Aoki and H. Otsuka, *Macromol. Rapid Commun.*, 2020, **41**, 1900460.
20 H. Sakai, T. Sumi, D. Aoki, R. Goseki and H. Otsuka, *ACS Macro Lett.*, 2018, **7**, 1359–1363.
21 H. Sakai, D. Aoki, K. Seshimo, K. Mayumi, S. Nishitsuji, T. Kurose, H. Ito and H. Otsuka, *ACS Macro Lett.*, 2020, **9**, 1108–1113.
22 Y. Mao, Y. Kubota, T. Kurose, A. Ishigami, K. Seshimo, D. Aoki, H. Otsuka and H. Ito, *Macromolecules*, 2020, **53**, 9313–9324.
23 Y. Mao, Y. Kubota, J. Gong, T. Kurose, A. Ishigami, K. Seshimo, T. Watabe, D. Aoki, H. Otsuka and H. Ito, *Macromolecules*, 2021, **54**, 8664–8674.
24 K. Seshimo, H. Sakai, T. Watabe, D. Aoki, H. Sugita, K. Mikami, Y. Mao, A. Ishigami, S. Nishitsuji, T. Kurose, H. Ito and H. Otsuka, *Angew. Chem., Int. Ed.*, 2021, **60**, 8406–8409.
25 D. Montarnal, M. Capelot, F. Tournilhac and L. Leibler, *Science*, 2011, **334**, 965–968.
26 J. M. Winne, L. Leibler and F. E. Du Prez, *Polym. Chem.*, 2019, **10**, 6091–6108.
27 Y.-L. Liu and T.-W. Chuo, *Polym. Chem.*, 2013, **4**, 2194–2205.
28 Y. Chen, Z. Tang, Y. Liu, S. Wu and B. Guo, *Macromolecules*, 2019, **52**, 3805–3812.
29 K. Yanada, S. Kato, D. Aoki, K. Mikami, H. Sugita and H. Otsuka, *Chem. Commun.*, 2021, **57**, 2899–2902.
30 K.-S. Focsaneanu, C. Aliaga and J. C. Scaiano, *Org. Lett.*, 2005, **7**, 4979–4982.
31 J. Slootman, V. Waltz, C. J. Yel, C. Baumann, R. Göstl, J. Comtet and C. Creton, *Phys. Rev. X*, 2020, **10**, 041045.